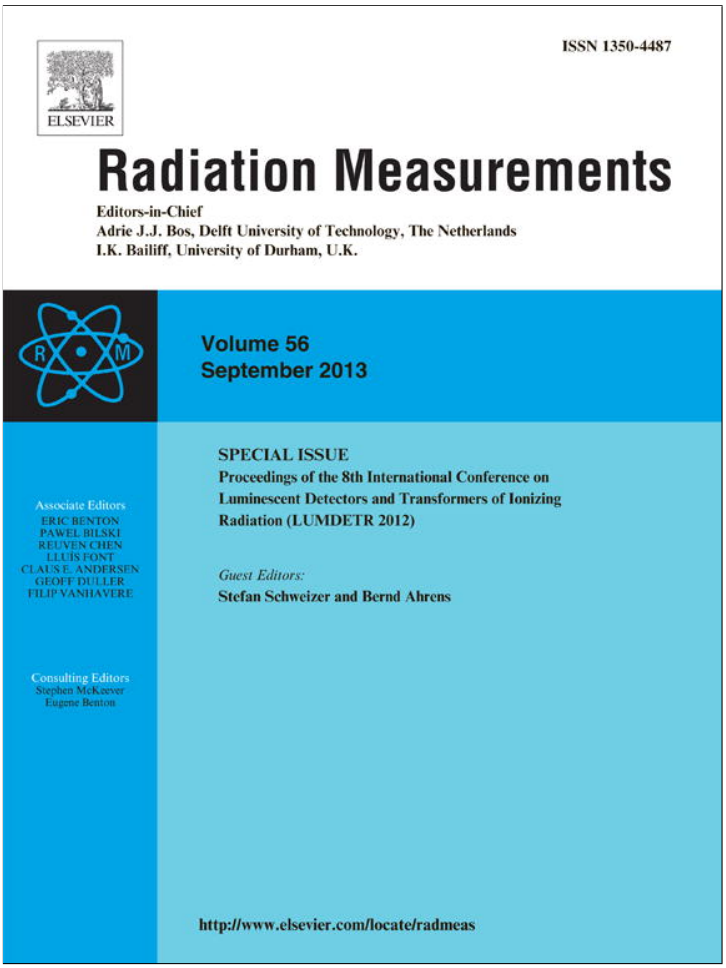

Radiation Measurements 56 (2013) 393–396

Contents lists available at SciVerse ScienceDirect

Radiation Measurements

journal homepage: www.elsevier.com/locate/radmeas

Intrinsic and impurity luminescence of rare earth ions doped KYF_4 nanophosphors

V.N. Makhov [a,*], A.S. Vanetsev [b,c], N.M. Khaidukov [b], M. Yin [d], X.T. Wei [d], A. Kotlov [e], A.N. Belsky [f]

[a] P. N. Lebedev Physical Institute, 53 Leninskii Prospekt, Moscow 119991, Russia
[b] N. S. Kurnakov Institute of General and Inorganic Chemistry, 31 Leninskii Prospekt, Moscow 119991, Russia
[c] Institute of Physics, University of Tartu, Riia 142, Tartu 51014, Estonia
[d] University of Science and Technology of China, Hefei 230026, PR China
[e] HASYLAB at DESY, Notkestraße 85, Hamburg 22607, Germany
[f] Institut Lumière Matière, UMR5306, CNRS, Université Claude-Bernard, Lyon 1, Villeurbanne F-69622, France

HIGHLIGHTS

- In KYF_4 hexagonal nanopowder an intense self-trapped exciton luminescence is detected.
- This excitonic luminescence in KYF_4 hexagonal nanopowders is not quenched at 300 K.
- Emission band of excitonic luminescence overlaps with Ce^{3+} and Tb^{3+} 4*f*-5*d* absorption.
- In hexagonal KYF_4 nanopowders an efficient energy transfer to Ce^{3+} and Tb^{3+} was found.

ARTICLE INFO

Article history:
Received 13 October 2012
Received in revised form
24 January 2013
Accepted 30 January 2013

Keywords:
Nanophosphors
Microwave-hydrothermal synthesis
Self-trapped excitons
Rare earth ions
KYF_4

ABSTRACT

The KYF_4 nanopowders, non-doped and doped with Ce^{3+} or Tb^{3+}, having well-crystallized, unaggregated, monodisperse (±15%) nanoparticles with the cubic (the size in the range from ~15 to ~30 nm) or hexagonal (from ~30 to ~50 nm) crystal structure have been successfully synthesized by microwave-hydrothermal treatment of as-precipitated gels. In KYF_4 hexagonal nanopowders an intense STE-type luminescence at ~4.4 eV was observed which is not quenched at room temperature. In contrast to single crystals or cubic nanopowders, in KYF_4 hexagonal nanopowders doped with Ce^{3+} or Tb^{3+}, a rather efficient energy transfer is observed from the host to Ce^{3+} or Tb^{3+} ions, respectively, because of overlapping the emission spectrum of STE-type luminescence and the spectrum of efficient absorption on 4*f*-5*d* transitions in Ce^{3+} or Tb^{3+}.

1. Introduction

In nanophosphors with reasonable sizes of nanoparticles (of the order of 10 nm or larger corresponding to typical penetration length of light for host absorption) the main spatial confinement effect on optical properties is due to the increase of surface area/volume ratio in nanoparticles, which leads to increased probability of near-surface nonradiative decay, and accordingly to smaller quantum yield (see, e.g. Tian et al., 2008). On the other hand, nanophosphors can exhibit novel properties compared to traditional luminescent materials. In particular, a change in the crystal structure of a nanosized material compared to the bulk one can result in strong variations of luminescence properties of the phosphor. For example, the bulk KYF_4 crystallizes in hexagonal phase (Le Fur et al., 1992) but nanosized particles of KYF_4 tend to crystallize in isotropic cubic phase due to lower specific surface energy (Ayyub et al., 1995).

In the present work, luminescence properties of nanosized KYF_4 powders undoped and doped with Tb^{3+} or Ce^{3+} have been studied under excitation by UV and vacuum UV (VUV) synchrotron radiation.

2. Experiment

KYF_4 nanopowders were synthesized by microwave-hydrothermal treatment of gels freshly precipitated from aqueous

* Corresponding author. Tel.: +7 499 1326575; fax: +7 495 9382251.
E-mail address: makhov@sci.lebedev.ru (V.N. Makhov).

1350-4487/$ – see front matter © 2013 Elsevier Ltd. All rights reserved.
http://dx.doi.org/10.1016/j.radmeas.2013.01.070

solutions. $Y(NO_3)_3 \cdot 6H_2O$ (Aldrich, 99.9% purity), $Ce(NO_3)_3 \cdot 6H_2O$ (Aldrich, 99.9% purity), $Tb(NO_3)_3 \cdot 5H_2O$ (Aldrich, 99.9% purity), $KF \cdot 2H_2O$ (KhimMed, 99.9% purity) and deionized water were used as starting compounds. Solution of 5 mmols in total of $Y(NO_3)_3 \cdot 6H_2O$ and $Ce(NO_3)_3 \cdot 6H_2O$ (or $Tb(NO_3)_3 \cdot 5H_2O$) with Y^{3+}:Ce^{3+} (or Tb^{3+}) ratio 98:2 in 10 ml of deionized water was prepared as well as solution of 20 (or 200) mmols of $KF \cdot 2H_2O$ in 30 ml of deionized water. After that solution of nitrates was added dropwise to solution of potassium fluoride under vigorous stirring. After preparation, the gels were heated in teflon autoclaves at 200 °C for 4 h using laboratory microwave-hydrothermal device (Berghof Speedwave-3M+, frequency 2.45 GHz, output power 1.2 kW).

Using different F^-:RE^{3+} molar ratio in initial solutions (4:1 and 40:1) KYF_4 nanoparticles with hexagonal and cubic structure, respectively, were obtained. It was shown in our previous paper (Makhov et al., 2012) that large excess of precipitant (F^-) in initial solution allows obtaining nanoparticles of metastable cubic phase using microwave-hydrothermal treatment. Transformation from hexagonal to cubic phase and back is an excellent example of size-dependent transformation (Ayyub et al., 1995). As the size of particles decreases, high surface energy triggers transformation from anisotropic hexagonal to isotropic cubic phase, which is characterized by lower surface energy. Addition of large excess of F^--ions in reaction mixture leads to increase of supersaturation. It is well known that with the increase of supersaturation the velocity of nucleation increases significantly sharper than velocity of growth. Thus, the large excess of F^--ions in the reaction mixture leads to formation of larger amount of smaller particles and therefore to stabilization of cubic phase.

The phase composition of synthesized samples was characterized by powder X-ray diffraction (XRD) analysis using Rigaku D/MAX 2500 diffractometer with Cu Ka (k = 1.5406 Å) radiation. Identification of diffraction peaks was carried out using JCPDS PDF2 database. The transmission electron microscopy (TEM) images of the samples were taken with Leo912 AB Omega microscope under accelerating voltage 100 kV. The pure and doped with Tb^{3+} or Ce^{3+} KYF_4 single crystals, used as reference samples, were synthesized by hydrothermal technique (Le Fur et al., 1992).

The luminescence spectroscopy experiments were carried out at the SUPERLUMI set-up of HASYLAB at DESY (Zimmerer, 2007) using synchrotron radiation from the DORIS storage ring for excitation. A 0.3-m Czerny-Turner monochromator-spectrograph SpectraPro-308i (Acton Research Inc.) supplied with fast microchannel-plate photomultiplier tube Hamamatsu R3809U-50 was used for the measurements of emission spectra in the spectral range of 200–700 nm, for selecting the monitored wavelength when measuring excitation spectra of emissions and for luminescence decay kinetics measurements. The time resolution of the detection system was ~100 ps with a 130 ps length of the exciting synchrotron radiation pulses followed with the period of 192 ns. Nanopowders were slightly pressed into small copper cups (with a diameter of 3 mm and thickness of 1 mm), which were then glued onto a copper sample holder of a flow-type liquid helium cryostat. The KYF_4 single-crystalline samples were grounded into powders prior to the mounting onto a sample holder.

3. Results and discussion

The KYF_4 powders, non-doped and doped with Ce^{3+} or Tb^{3+}, having well-crystallized, unaggregated, monodisperse (±15%) nanoparticles with the cubic (the size in the range from ~15 to ~30 nm) or hexagonal (from ~30 to ~50 nm) crystal structure have been synthesized. Concentration of the doping Ce^{3+} or Tb^{3+} ions was ~2.0 mol%. Examples of XRD patterns and TEM images of synthesized powders are shown in Figs. 1 and 2. It can be seen that samples with cubic structure are almost free from hexagonal phase. Unfortunately for samples with hexagonal structure it is hard to make similar conclusion since all peaks corresponding to cubic phase are very close to the ones of hexagonal phase.

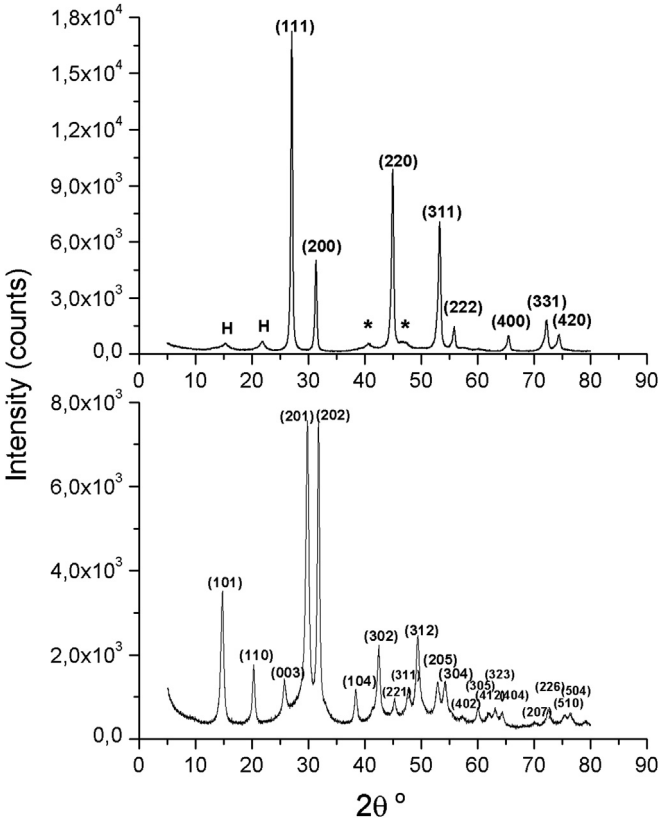

Fig. 1. XRD of cubic (upper) and hexagonal (lower) KYF_4:Ce^{3+} nanopowders with average particle sizes 19 and 36 nm respectively.

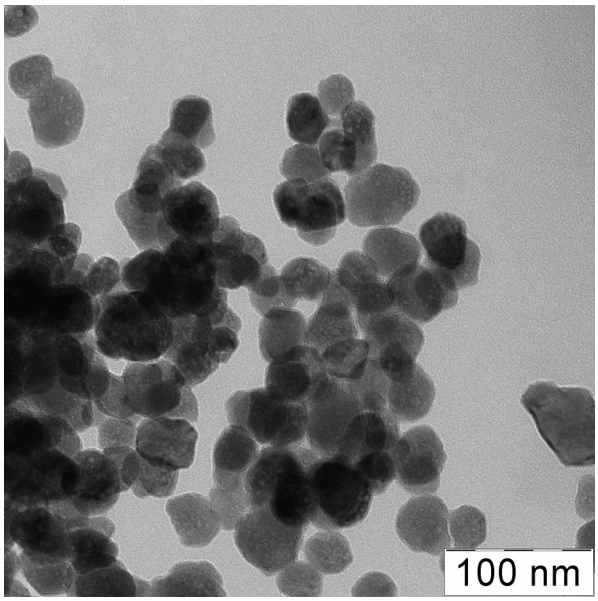

Fig. 2. TEM images of hexagonal KYF_4:Ce^{3+} nanopowders with average particle size 36 nm.

One may notice that despite larger size of particles of hexagonal phase observed by means of TEM comparing to particles of cubic phase, XRD peaks of hexagonal phase have lower intensity and are significantly broadened. This result allows making a suggestion that for some reason the crystallinity of hexagonal particles is lower comparing with cubic particles. One of the possible explanations for this result is that formation of hexagonal phase partially or entirely proceeds through formation of nuclei of cubic phase, which later transform to hexagonal phase. Even after complete transformation the low ordered zones can still remain available as the processes of crystallization and ordering are rather slow at temperatures of synthesis.

It is necessary to mention that the actual positions of the peaks in the obtained XRD patterns for non-cubic samples slightly shift with changing the particle size, i.e. there is always noticeable difference between experimental XRD pattern and the XRD pattern from the database for hexagonal KYF_4. For several samples the XRD pattern can be fitted well enough as superposition of the patterns for cubic KYF_4 and KY_3F_{10} phases. However, the formation of such a KF-deficient phase as KY_3F_{10} during cubic-to-hexagonal transformation of KYF_4 phase can be hardly expected. On the other hand, the appearance of some intermediate phase on the stage of transformation from cubic to hexagonal phase with crystal structure similar to that of KY_3F_{10} is possible. This can explain the moderate-quality coincidence with the data from XRD database.

As has been shown recently (Makhov et al., 2012), the synthesized nanopowders with the hexagonal structure show rather intense broadband luminescence (at ~4.4 eV at room temperature), which is efficiently excited in the region around the edge of intrinsic absorption of the host and is only slightly quenched at room temperature (Fig. 3).

The shape of the excitation spectrum of this emission is similar to that of self-trapped exciton (STE) luminescence from a KYF_4 single crystal with a dip at ~11.0 eV, which is usually ascribed to near-surface losses of excitations in the peak of excitonic absorption, although for nanopowders the excitation spectrum is much broader. The observed properties of this UV emission can be well explained within the model of luminescence from "near-defect STEs". The nature of this STE-type luminescence in hexagonal KYF_4 nanopowders is still under discussion. As the phase transition from metastable cubic to stable hexagonal phase of KYF_4 is induced by the growth of nanoparticles, our hypothesis is that forming hexagonal nanoparticles still contain small inclusions of cubic phase undetectable by XRD analysis. These inclusions can be small-sized core of cubic phase surrounded by massive shell of hexagonal phase or very small cubic phase nanoparticles, incorporated in aggregates of larger nanoparticles of hexagonal phase and, therefore, protected from the growth and transformation. Similar effect of the presence of cubic core inside nanoparticles of hexagonal phase was observed, for example, in ZnO (Ding et al., 2007). Excitons created in hexagonal nanoparticles can become trapped near such defects of crystal structure. Our experimental results have shown that the smaller is the mean size of nanoparticles of hexagonal KYF_4 phase in synthesized nanopowder the higher is the intensity of this specific luminescence. This can be understood if one assumes that the relative volume of inclusions of cubic phase in nanoparticles of hexagonal phase increases if the size of these nanoparticles is close to the critical one corresponding to the cubic–hexagonal phase transition. Anyway, additional studies are needed for clarifying the mechanism of this luminescence and the nature of defects involved. In particular, the presence of the third, "intermediate" phase with crystal structure different from both cubic and hexagonal phase, which is responsible for this specific luminescence, can be also considered.

For Ce^{3+} doped samples it was found that in contrast to KYF_4:Ce^{3+} single crystals or cubic nanopowders, the intensity of Ce^{3+} 5*d*-4*f* luminescence in hexagonal KYF_4:Ce^{3+} nanopowders is considerably increased (also at room temperature) under excitation in near-excitonic region $h\nu = 10–12$ eV (Fig.4). In this spectral region the shape of excitation spectrum of Ce^{3+} 5*d*-4*f* luminescence in hexagonal KYF_4:Ce^{3+} nanopowder is very similar to the shape of excitation spectrum of excitonic luminescence in undoped hexagonal KYF_4 nanopowder with the onset at $h\nu \sim 9.5$ eV. This effect is due to the fact that in hexagonal KYF_4:Ce^{3+} nanopowder a rather efficient energy transfer from STE-type centres to Ce^{3+} ions is observed because of overlapping the emission spectrum of STE-type luminescence and the spectrum of efficient absorption on 4*f*-5*d* transitions in Ce^{3+} (see Fig. 4).

Under Ce^{3+} 4*f*-5*d* excitation (at ~4.3 eV) in hexagonal KYF_4:Ce^{3+} nanopowders the Ce^{3+} 5*d*-4*f* luminescence is practically not quenched and has a bit longer decay constant than that of single-crystalline sample showing decay with $\tau = 33$ ns (Fig.5). Under excitation in excitonic region (at $h\nu = 10–12$ eV) the decay of Ce^{3+} 5*d*-4*f* luminescence in hexagonal KYF_4:Ce^{3+} nanopowder

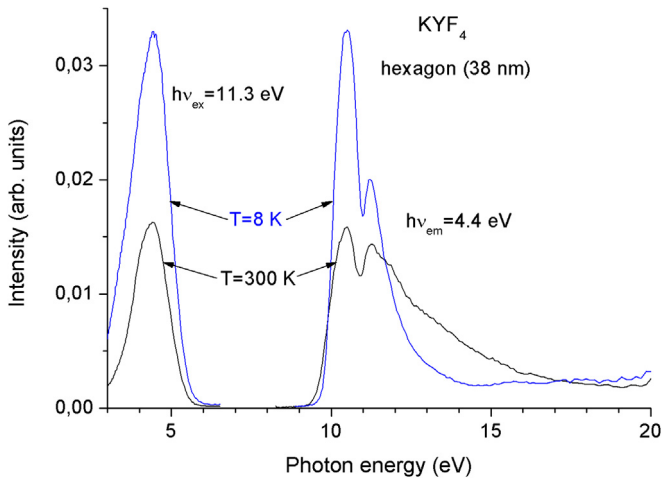

Fig. 3. Emission spectra under excitation at 11.3 eV (left) and excitation spectra of emission at 4.4 eV (right) for undoped hexagonal KYF_4 nanopowder at 300 and 8 K.

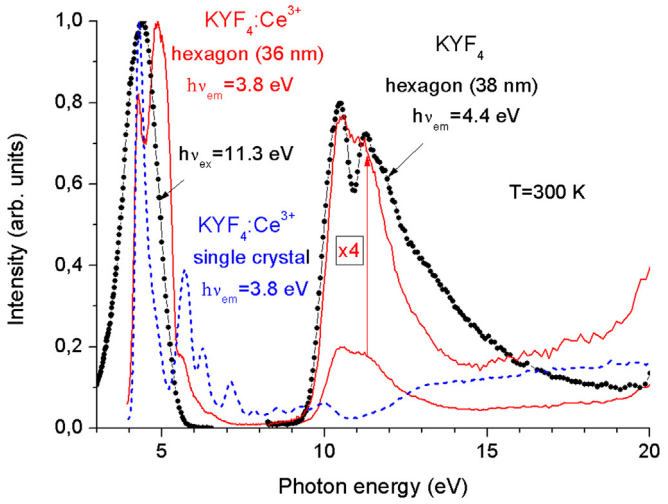

Fig. 4. Emission (under excitation at 11.3 eV) and excitation (for emission at 4.4 eV) spectra of STE-type luminescence in undoped hexagonal KYF_4 nanopowders (dotted lines) and excitation spectra of Ce^{3+} 5*d*-4*f* luminescence (at 3.8 eV) in hexagonal nanopowder (solid line) and single crystal (dashed line) of KYF_4:Ce^{3+}.

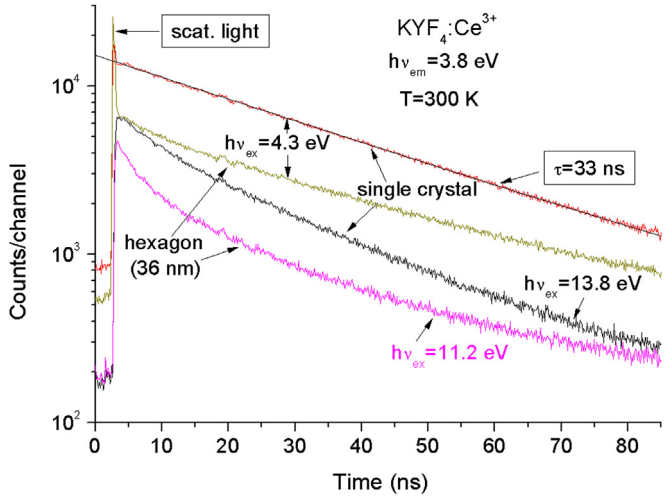

Fig. 5. Decay curves of Ce^{3+} 5*d*-4*f* luminescence (at 3.8 eV) in hexagonal nanopowder and single crystal of KYF_4:Ce^{3+} under Ce^{3+} 4*f*-5*d* excitation (at ~4.3 eV) and host excitation (at 11.2 eV for nanopowder and at 13.8 eV for single crystal).

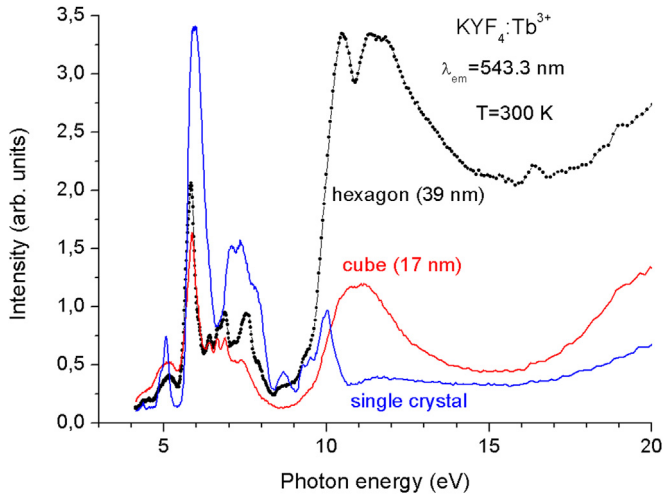

Fig. 6. Excitation spectra of Tb^{3+} $^5D_4$–$^7F_5$ luminescence at 543.3 nm for cubic and hexagonal nanopowders and single crystals of KYF_4:Tb^{3+}.

becomes non-exponential thus showing the presence of some quenching. However the intensity of Ce^{3+} 5*d*-4*f* luminescence under excitation in this spectral region is much higher than in the case of single crystalline sample or cubic nanopowders.

For Tb^{3+} doped samples it was found that Tb^{3+} 4*f*-4*f* luminescence in hexagonal KYF_4:Tb^{3+} nanopowders is also excited efficiently in the region above the edge of intrinsic absorption of the host, and also in contrast to single crystals or cubic nanopowders (Fig.6). This effect has the same nature as in Ce^{3+} doped samples and is due to overlapping of emission spectrum of STE-type centres in hexagonal KYF_4 nanopowders with the edge of absorption on 4*f*-5*d* transitions in Tb^{3+} although for Tb^{3+} ions overlapping is with absorption band corresponding to weaker spin-forbidden 4*f*-5*d* transitions at ~5 eV.

The support of the model suggesting the existence of the cubic core or clusters inside hexagonal nanoparticles can be found by comparison of the shapes of excitation spectra of Tb^{3+} luminescence for these three types of samples. The excitation spectrum for hexagonal nanopowder in the near-excitonic region (10–12 eV) looks as superposition of excitation spectra for single crystal (having hexagonal structure) and cubic nanopowder.

4. Conclusions

In KYF_4 hexagonal nanopowders an intense STE-type luminescence at ~4.4 eV is observed which is not quenched at room temperature. In contrast to single crystals or cubic nanopowders, in KYF_4 hexagonal nanopowders doped with Ce^{3+} or Tb^{3+}, a rather efficient energy transfer is observed from the host to Ce^{3+} or Tb^{3+} ions, respectively, because of overlapping the emission spectrum of STE-type luminescence and the spectrum of efficient absorption on 4*f*-5*d* transitions in Ce^{3+} or Tb^{3+}.

Acknowledgements

This work was supported by European Community's Seventh Framework Programs FP7/2007-2013 under grant agreement n° 312284 and FP7-INCO-2010-6-1 under grant agreement n° 266531 (project SUCCESS). The support by the BMBF Grant RUS 10/037, RFBR Grant 13-02-91179, NSFC Grants 11074245 and 11011120083 is also gratefully acknowledged.

References

Ayyub, P., Palkar, V.R., Chattopadhyay, S., Multani, M., 1995. Effect of crystal size reduction on lattice symmetry and cooperative properties. Phys. Rev. B 51, 6135–6138.

Ding, Y., Wang, Z.L., Sun, T., Qiu, J., 2007. Zinc-blende ZnO and its role in nucleating wurtzite tetrapods and twinned nanowires. Appl. Phys. Lett. 90, 153510–153513.

Le Fur, Y., Khaidukov, N.M., Aleonard, S., 1992. Structure of KYF_4. Acta Crystallogr. C. 48, 978–982.

Makhov, V.N., Vanetsev, A.S., Khaidukov, N.M., Belsky, A.N., Yin, M., Wei, X.T., Kotlov, A., 2012. Crossluminescence of nanosized KYF_4. IEEE Trans. Nucl. Sci. 59, 2102–2105.

Tian, L.J., Sun, Y.J., Yua, Y., Kong, X.G., Zhang, H., 2008. Surface effect of nanophosphors studied by time-resolved spectroscopy of Ce^{3+}. Chem. Phys. Lett. 452, 188–192.

Zimmerer, G., 2007. Superlumi: a unique setup for luminescence spectroscopy with synchrotron radiation. Radiat. Meas. 42, 859–864.